Characterization of Structural Vibration and Acoustic Radiation with a Beam-Array Doppler Vibrometer

Vladimir B. Markov[1]
Advanced Systems & Technologies, Inc., Irvine, CA 92618

William M. Humphreys, Jr.[2]
NASA Langley Research Center, Hampton, Virginia 23681

Anatoliy I. Khizhnyak[3]
Advanced Systems & Technologies, Inc., Irvine, CA 92618

This paper discusses the operational principles of an assembly of two opto-electronic modules with their configurations based on a Laser-Array Doppler Vibrometer (LADV) and a Shack-Hartmann Wavefront Sensor (SHWFS). Both sensors can operate concurrently providing complementary data. While the SHWFS is a well-established system that enables low-bandwidth spatio-temporal characterization of aerodynamic turbulence, the LADV technology allows real-time detection of structural vibrations and associated acoustic radiation fields. Practical examples are shown of the instruments' capabilities, focusing on the ability to simultaneously capture, visualize and quantitatively characterize full-field non-stationary structural dynamics and unsteady sound fields or transient flow fields around ground test facility airframe models or other structures of interest. The parallel multi-channel architecture of the LADV system enables synchronous detection and temporal correlation of indicators related to the spatio-temporal vibration of the structure under inspection. This unique feature is essential for real time detection and categorization of the structural and acoustic dynamics of transient events. For the present study, the LADV data have been successfully compared with measurements obtained with the SHWFS in the wake of a subsonic scale-model airfoil. The ability of the LADV-SHWFS coupled measurements to perform real time non-intrusive evaluation and characterization of dynamic processes at operationally relevant bandwidths should provide a deeper insight into the complex structural dynamics that contribute to radiated sound fields.

I. Introduction

NASA has an enduring interest in the understanding of vibroacoustics (i.e., structural acoustics) as applied to airframes and launch vehicles. Understanding fluid-structure interactions is a critical area for numerical modelers employing finite element and boundary element methods. This requires the development of analysis tools for characterization of the vibroacoustic response of structural components and assemblies as well as measurement of the associated acoustic radiation field to establish causality between the vibrating structure and the radiated field. Measurement and analysis tools covering middle and high frequencies are of particular interest to modelers [1-3].

Researchers have traditionally collected structural acoustic data using point laser vibrometers, intensity scanners, and individual point accelerometers. The existing technologies employed to interpret the relationship between structural vibrations and the sound fields they produce, such as near field acoustic holography [4], or more recent beam-forming methods [5-7] use an inverse approach to assess the problem. Put another way, these techniques require the pressure sensor or microphone arrays to measure the radiated sound field and use this data to reconstruct images of the apparent noise source via inverse computational methods. However, the radiated sound fields, from

[1] President, Advanced Systems and Technologies, Inc.
[2] Aerospace Engineer, Advanced Measurement and Data Systems Branch, Associate Fellow AIAA.
[3] Chief Scientist, Advanced Systems and Technologies, Inc.

which these images are generated, constitute only one component, and more often a fraction, of the total energy transport and conversion mechanisms from which they arise. In addition to being intrusive these evaluation techniques are bandwidth limited, time consuming to implement, and require extensive data processing. Furthermore, limitations of the spatio-temporal bandwidth can generate false results in the form of pseudo (noise) sources, making an accurate appraisal of abatement system efficacy difficult.

This paper discusses the use of paired non-contact optical measuring techniques that enables direct detection of the full-field non-stationary dynamics of structural vibrations and the flow fields around a scaled model wing. In particular, it addresses the fundamental lack of a comprehensive non-invasive test methodology to assess the complex and interdependent nature of non-stationary structural vibrations driven by the unsteady flow field. The methodology presented here provides the ability to characterize the role of aeroacoustics phenomena as a source of the noise and can establish causality between the structural vibration modes and acoustic radiation fields. The technologies used for this study consist of two complementary techniques: (i) a Laser-Array Doppler Vibrometer (LADV) to enable measurement of structural vibration modes and associated radiated sound fields, and (b) a Shack-Hartmann Wavefront Sensor (SHWFS) that enable characterization of the spatial dynamic flow around the test model in the wind tunnel.

The capacity of the LADV-SHWFS coupled measurement technique to perform a real time non-intrusive evaluation and characterization of the dynamic processes at operationally relevant bandwidths should provide a deeper insight into the complex structural dynamics that contribute to the radiated sound field. The operational capabilities of the LADV-SHWFS system and associated data can support an analysis of energy transfer and coupling mechanisms between different airframe mounted sub-structures, providing a diagnostic tool for identifying the contributory sources of structural vibration and aero-elastic generated noise. In effect, the test and evaluation capabilities of the merged LADV-SHWFS technique will aid next generation airframe designs and enhance flight performance and safety.

II. Assessment of Vibroacoustics and Airflow Dynamics

The experimental studies reported in this paper were performed using a setup that integrates on a single measuring platform two sensors, i.e. a Laser-Array Doppler Vibrometer and a Shack-Hartmann Wavefront Sensor as illustrated in the schematic shown in Fig. 1. These two sensor systems provide operational orthogonal data while being coupled through a single source representing the interface of the flow and the wing. As the LADV and SHWFS measuring units operate concurrently, the sets of data they provide are complimentary with one defining the vibrational dynamics of the wing impacted by the airflow, and the second one defining the spatial structure and dynamics of the airflow around the model in the wind tunnel.

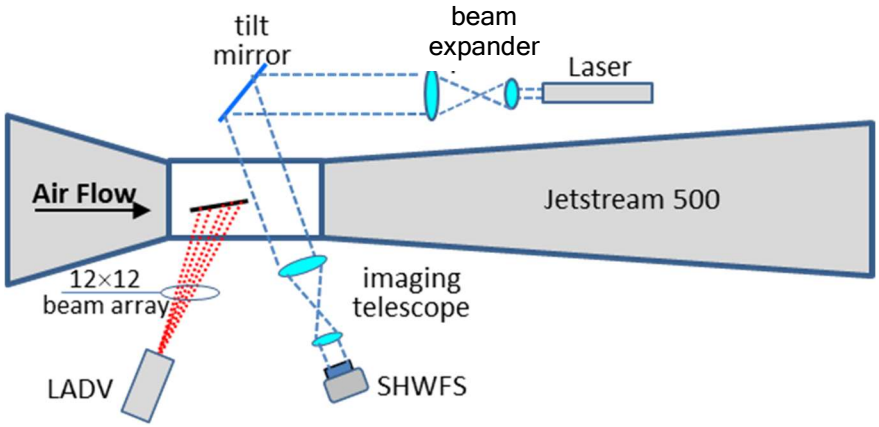

Figure 1. Optical configuration with the two sensors shown for measurement of vibro-dynamic (LADV) and spatio-temporal (SHWFS) modes.

A small-scale subsonic Jetstream 500 wind tunnel with a 5 1/4" square (13.3 cm square) by 16" (40.6 cm) long test section was used in these experimental studies. This tunnel can produce freestream velocities covering a range of 1.00 to 80.00 MPH (0.45 to 35.76 m/s). The test section has a high degree of optical access due to its transparent (Perspex) walls and mirrored base section, making it well suited for optical probing of the airflow. Test airfoil models can be attached horizontally to the fitted base mount that provides precision strain gage sensors to measure lift and drag forces. The tunnel speed is measured and controlled via a pitot tube with 0.1 MPH (0.05 m/s)

resolution. These data are collected by a microprocessor with a 12 bit A/D converter and displayed in Metric or English units.

For the investigations addressed in this paper, the LADV probe input-output optical zoom was adjusted such that the 12×12 beam array illuminated an area of 44 × 44 mm (with a 4-mm distance between measurement points) on a target set at about 500 mm away from the optical probe's objective. The pattern of the beam array can be matched to the spatial resolution anticipated in various tests and experiments.

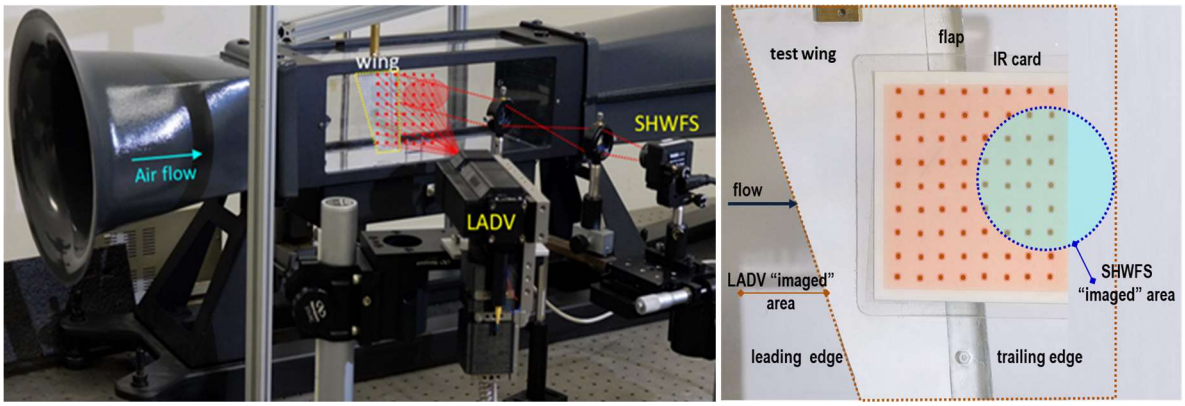

(a) (b)

Figure 2. Experimental setup for a dual LADV-SHWFS platform for characterization of full-field non-stationary structural dynamics and unsteady sound fields or transient flow. (a) Photo of overall setup; (b) Measurement zone geometry

Fig. 2 illustrates the experimental setup with a simple NACA wing model mounted in a top-down vertical configuration inside the test section of the tunnel. To physically isolate the impact of the airflow on the wing supporting post, the frame was dropped through the roof of the tunnel (seen in the figure). Such an arrangement is optimum to measure the airflow and acoustic fields around the leading and trailing edges of the model in addition to ensuring that the wing was isolated from vibrations of the tunnel walls and support system. A short section of the test article used in these experiments was 3D printed.

A. LADV Architecture and Setup

The architecture and integration of the laboratory version of the LADV comprises hybrid fiber-optics and free-space optical components. Specifically, the LADV architecture represents a modular design that integrates two key sub-modules, namely a probe head (Fig. 3 - top) and the support elements of the system, including: (i) a compact 2 watt CW fiber laser operating at a wavelength of 1550 nm; (ii) signal receivers coupled with data processing boards, and (iii) a small form factor computer to control system operation. The probe head integrates: (i) a compact fiber-optics coupled waveguide modulator for FM carrier generation; and (ii) a passive focal plane receiver that consists of a 2D micro-lens/fiber 12×12 array to convey optical signals from the LADV sensor-head to the system processor [8-9]. The fiber-optics architecture of the LADV enables a compact, robust and largely electromagnetic neutral probe, since the laser source, housed with the processor module, is fiber guided to the probe, while the 2D optical signals are fiber guided from the probe to the processor.

For this study, a deployed flap was added to the airfoil shown in Fig. 2(b). The angle of attack was set at 5 degrees and the beam-array spacing (Fig. 3 – bottom) could be changed from 2 mm to 5 mm depending upon the distance of the LADV probe head to the

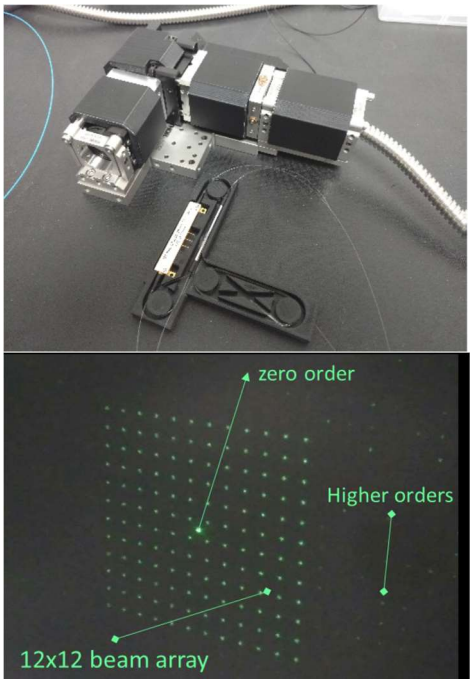

Figure 3. LADV probe head and beam geometry.

measurement region within the tunnel test section. Structural vibration measurements, modal behavior and associated acoustic noise caused by turbulence generated by the airfoil were acquired at various freestream velocities spanning a range of 20 mph (8.9 m/s) to 80 mph (35.7 m/s) within the tunnel operational specifications.

As shown in Fig. 2(a), the LADV probe head was placed outside of the wind tunnel on an angle/position-adjustable support during testing. For this study the angle of attack of the LADV beam-array was approximately 25 degrees with respect to the airfoil and approximately 20 degrees with respect to the test section windows. This latter angle is essential to prevent the window-returned light from propagating back to the LADV probe. With the total number of beams in a 12×12 array equal to 144 and the spacing of the beams at the measurement (airfoil) plane close to 4 mm, approximately 80 beams were placed on the wing and the remaining 64 beams were directed in front of the leading edge of the wing (see Fig. 2b). The back-scattered light from the airfoil surface and the surrounding area was collected by the same emitting-receiving optics of the LADV probe head, and once captured were delivered by the fiber array to the receiver through a fiber-optics umbilical for posterior parallel processing.

The LADV operational software is a critical component of the system used to provide processing, analysis and interpretation of the retrieved data. Following demodulation of the raw heterodyne data volume generated by the interferometer array, the software facilitates efficient and rapid review of the spatio-temporal or 4D set of data and provides the ability to extract unambiguously the specific events of interest. Review of this information supports data analysis and subsequent interpretation of the primary phenomenon being measured by the system. The data processing and analysis software can support 2D and 3D displays of the measured surface displacement and velocity data in both the time and frequency domains (Fig. 4). The Graphic User Interface (GUI) enables various filter settings and other parameters to be set to focus on specific features of interest in addition to enabling animations of the 3D or 2D data in the time or frequency domain to study temporal or spectral evolution of the data.

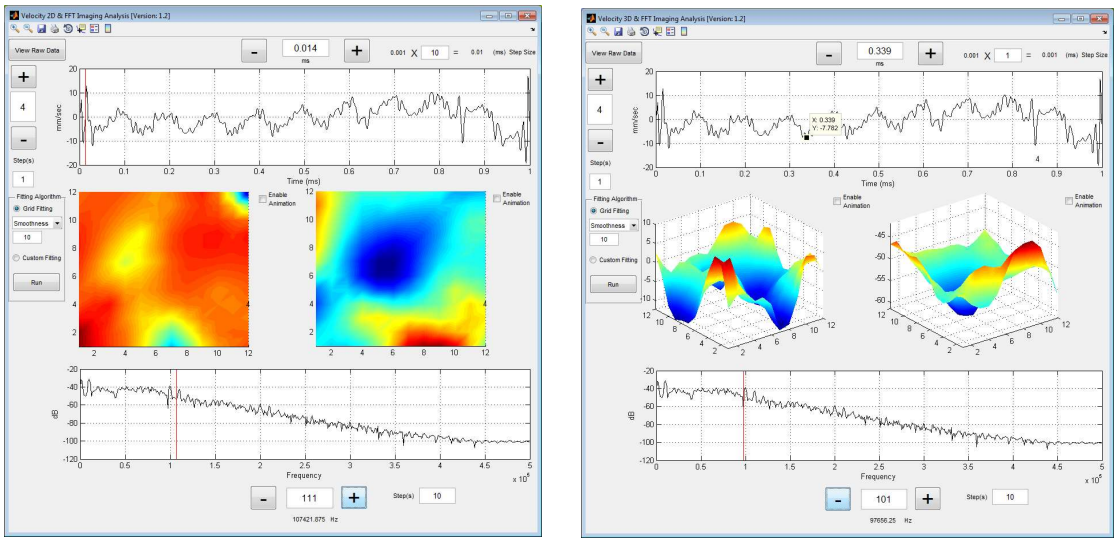

Figure 4. Graphical User Interface (GUI) for review and analysis of the LADV derived data.

B. Spatial Sensor Setup

In order to obtain concurrently with the LADV data the dynamics of the airflow in the region immediately downstream of the wing flap, the SHWF sensor was placed in the posterior zone of the airfoil, thus allowing the detection of aberrations in the wavefront of the transmitted laser beam caused by spatio-temporal non-uniformities in the flow. The wavefront sensor was placed to look through the wind tunnel test section in the area behind the airfoil trailing edge. Because of the limitations of the setup only a segment of the trailing edge area was exposed to the SHWF sensor. The optical layout of the spatial mode sensor is shown in Fig. 1. The key element of the spatial mode SHFW sensor is a high-speed Thorlabs wavefront detector (WFS20-7AR) with its design based on the Shack-Hartmann configuration. In the schematic shown in Fig. 1, the laser beam is expanded using a beam expander to a diameter ∅ = 2.0 cm and is then passed through the test section next to the airfoil flap. The transmitted beam is then collected by a telescope that reduces the diameter of the transmitted beam to match the size of the SHWF sensor with dimensions of 7.20 × 5.40 mm, consisting of 1440×1080 pixels set behind a 47×35 lenslet array. For this study, a Ne-Ne laser operating at a wavelength of λ= 633 nm (or an equivalent LED source) was utilized as the light

source. The sensor enables a wavefront sensitivity of λ/100 rms (root mean squared) at a frame rate up to 880 Hz. The temporal resolution (frame rate) of the available SHWF sensor limits the freestream velocity measurement range to values less than 35 mph (15.6 m/s); however, a high speed Shack Hartmann with a design based on the use of position sensitive detectors and operating at frequency up to 100 kHz has been experimentally demonstrated [11].

III. Experimental Results

A. Modal Identification by Swept Frequency Excitation

Fig. 5(a) illustrates a velocity profile for one LADV channel located on the airfoil with the most prominent surface velocity FFT peaks shown in Fig. 5(b). The resonant modes are identified in both the temporal and frequency domains at 28.5 Hz, 155 Hz, 167 Hz, 305 Hz, 410 Hz and 460 Hz.

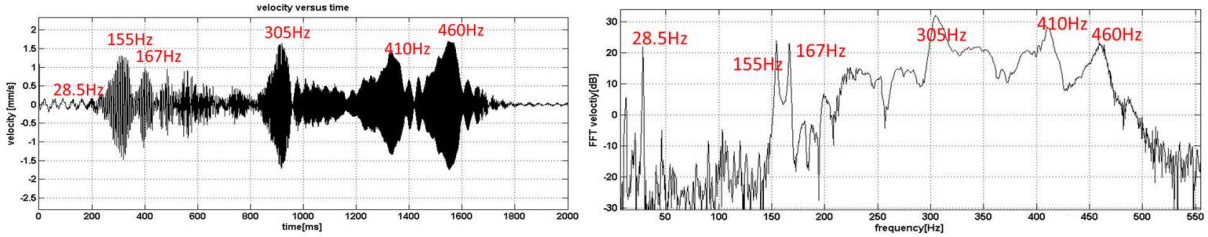

(a) (b)

Figure 5. Selected LADV channel velocity profile and prominent velocity FFT peaks for mode identification.

Fig. 6 illustrates measured surface velocity modal behavior for the airfoil for the fundamental mode at 28.5 Hz, as well as for the 155 Hz, 167 Hz and 410 Hz modes. All of these were identified both experimentally and by finite element (FE) calculations. The images are snapshots from full-field dynamic spatio-temporal and spatio-spectral 2D velocity images.

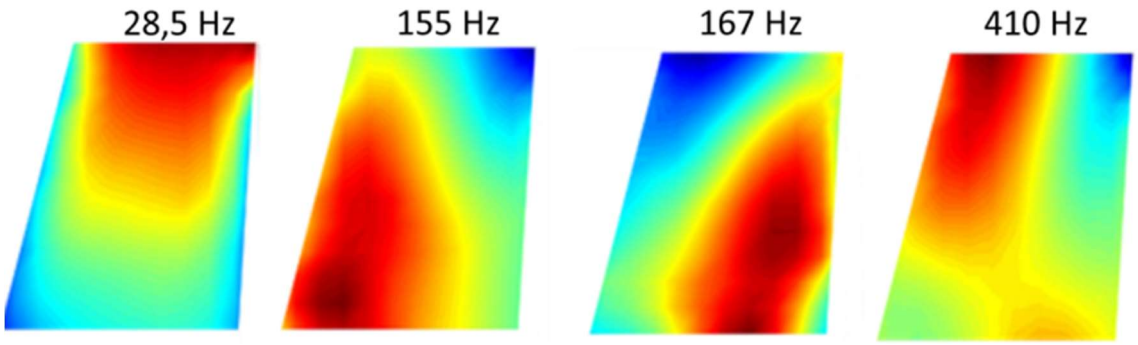

Figure 6. Measured Modal behavior of the tested airfoil.

Animated data ("movies") collected by the LADV also reveal the structural dynamics to include normal modes, coupled (closely-spaced) modes, modal coalescence, non-degeneracy, transient phenomenon and travelling waves showing the flow of energy across the structure. Frequency domain analyses (spatio-spectral velocity maps) indicate modal dispersion while further examination of the animated 2D temporal velocity profiles also disclose rapid spatial rotations of the normal mode velocity distributions as the forced excitation sweeps through the resonant peak. This effect is due to non-degeneracy or mode-splitting, which is commonly associated with a non-uniform imbalance in the mass distribution of a centro-symmetric solid body structure.

B. Real-time Acoustic/Flow Field Visualization by Constant Phase Optical Path Integration

A velocity-time profile and its corresponding FFT for selected channel number 1 in the LADV beam array are shown in Fig. 7 for measurements conducted downstream of the airfoil trailing edge at a free stream speed of

72 mph (32.2 m/s). The corresponding velocity FFT maps are illustrated in Fig. 8. Note that the spectral content of the flow is similar to the modal frequencies identified for the flap during the structural vibration measurements.

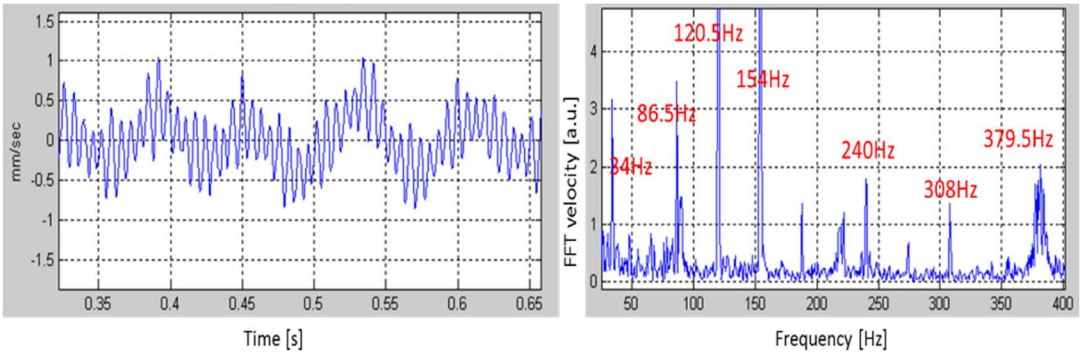

(a) (b)

Figure 7. Constant phase integrated optical path measurements in trailing edge flow at a freestream velocity of 32.2 m/s for LADV channel 1.
a) velocity-time profile illustrating modal coalescence of 34 Hz, 120.5 Hz and 154 Hz modes
b) velocity FFT showing most prominent peaks.

A qualitative, dynamic, real-time visualization of flow field dynamics behind the airfoil's trailing edge have been also recorded for a tunnel speed of 72 mph (32.2 m/s). Further examination of the animated data (not shown here) demonstrates the existence of a coalescence of different modes, as for example the ones identified at frequencies of 28.5 Hz, 85.8 Hz, 149 Hz, or at a different moment in time the coexistence of 85.8 Hz, 120.5 Hz and 149 Hz frequencies.

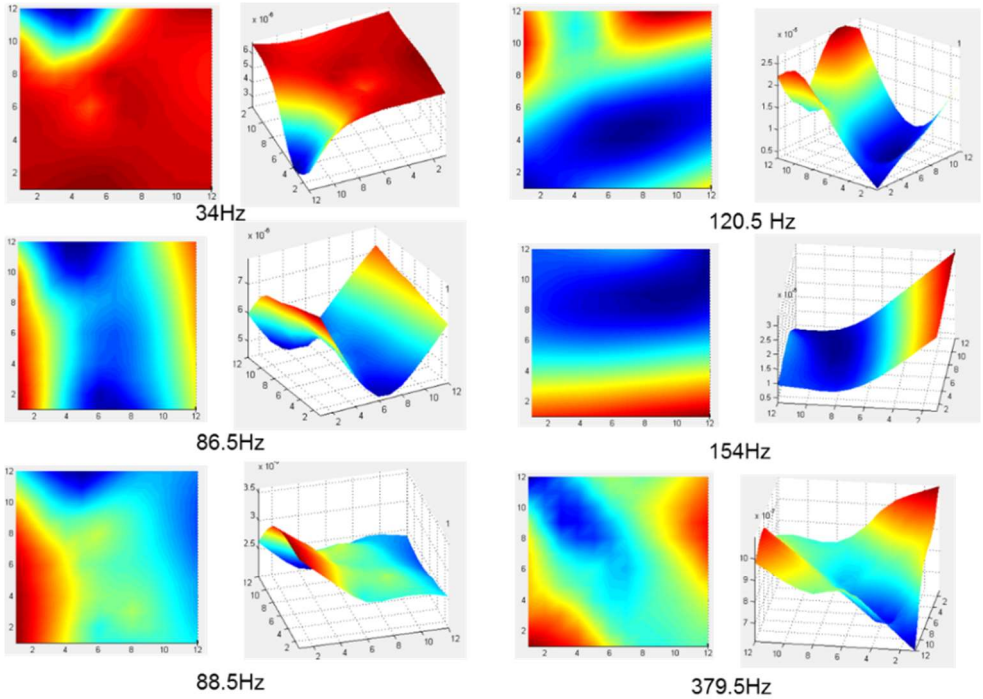

Figure 8. 2D and 3D velocity FFT maps captured by constant phase integrated optical path measurements performed in the wind tunnel, behind the airfoil's trailing edge at a freestream velocity of 32.2 m/s.

Correlations between the vibrational spectra of the airfoil and the dynamics of the airflow behind the wing's trailing edge at a freestream velocity of 54 mph (24.2 m/s) are illustrated in Fig. 9. Here panel (a) outlines the temporal dynamics of the wing captured by channel 4 of the LADV beam array, and panel (b) corresponds to LADV channel 68 that passes through the airflow behind the wing's trailing edge. The specifications of the data shown in Fig. 9 are as follows:

(a1) – the dynamics of the normal component of wing's surface velocity (channel 4);
(a2) – the expanded pattern of the surface velocity of the wing between 810 ms and 990 ms from (a1);
(a3) – the spectra of wing surface vibrational dynamic with resonant frequencies;

(b1) – the normal component of the airflow velocity in the vortex behind the trail edge (channel 68);
(b2) – b1 expanded between 810 ms and 990 ms;
(b3) – the resonant spectra of the perturbed airflow behind the wing's trailing edge.

The data shown in Fig. 9 demonstrate clear correlation of the perturbed air flow behind the wing's trailing edge with the surface vibrational parameters for the wing. However one should bear in mind that in general the true characteristics of such dynamic processes should account for the vibrational characteristics of the wind tunnel's test chamber perplex windows as well as boundary layers along the windows as discussed in [9].

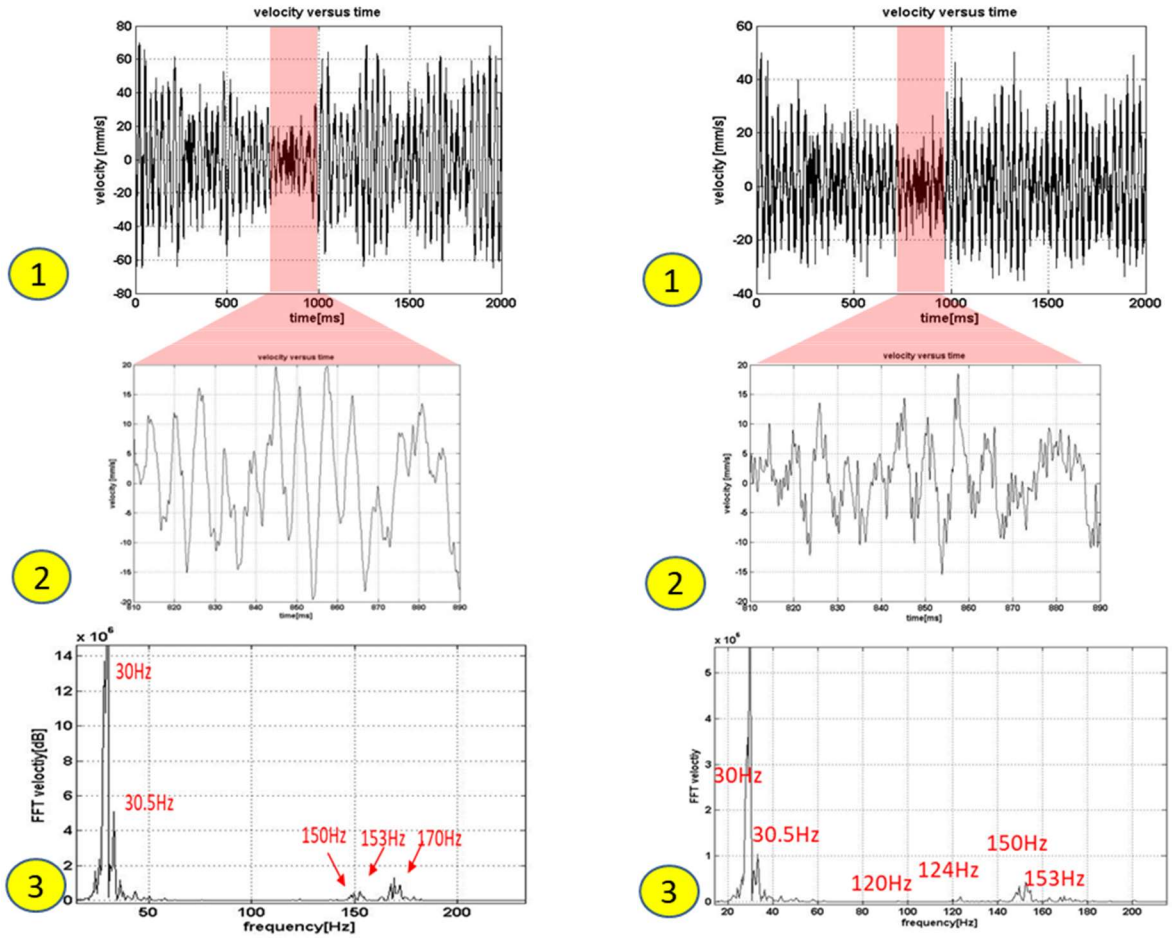

a) **b)**

Figure 9. Localized vibroacoustic spectra captured on (a) the airfoil surface and (b) downstream of airfoil trailing edge.

Parallel with the LADV-based measurements of the vibrational dynamics associated with the airfoil in the tunnel, the spatial dynamics of the airflow downstream of the model trailing edge were measured and characterized using the SHWF sensor system. The measurements were band limited to the dynamic range of the currently available WFS20-7AR sensor and compared with the data taken with the LADV as illustrated in Fig. 10. Here Fig. 10(a) shows the position of the wing trailing edge, Fig. 10(b) depicts a typical pattern of the path-integrated perturbations in the airflow detected with the Shack-Hartmann wavefront sensor, and Fig. 10(c) shows the results of the measurements with the LADV. The instantaneous whole-field pattern of the airflow perturbations seen in Fig. 10(b) and Fig. 10(c) correlates well with the data for channels 4 and 68 in Fig. 9 (a2) and (b2) and their related spectra in (a3) and (b3) in that figure.

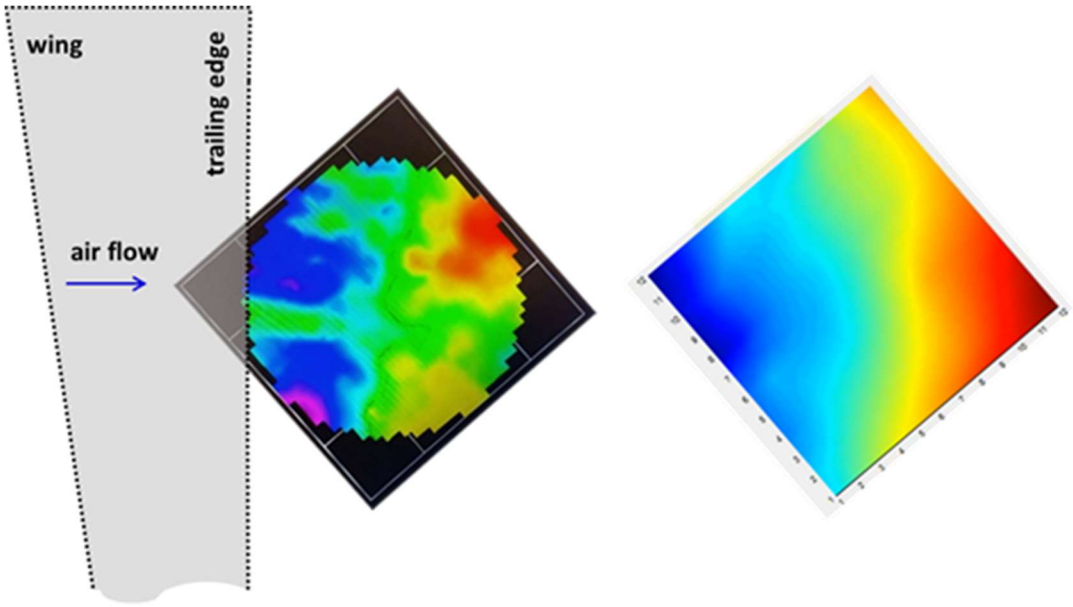

Figure 10. Imaging of the perturbed airflow behind the trailing edge of the wing. (a) outline of airfoil geometry; (b) measured with SHWF sensor; (c) measured with LADV

IV. Conclusion

This work demonstrates a new capability for real-time, full-field: (i) quantitative measurements of flow induced structural vibrations including mode coalescence and splitting, and (ii) visualization of the flow field around a test article's edges situated in a small scale wind tunnel operated at speeds up to 80 mph (35.8 m/s). The LADV instrument is capable of simultaneous measurement of surface velocities at 144 discrete measurement locations, allowing for the detection of temporally resolved, evolving modal structures on the model surface. The SHWF sensor provides the capability of detecting in real time path-integrated laser beam wavefront disturbances generated by fluctuating disturbances in an airflow under study. The results obtained using both the LADV and SHWF sensor simultaneously on a scaled airfoil section in a small subsonic wind tunnel establish that the LADV-SHWFS dual sensor technique is able to rapidly acquire various elements of the modal dynamics of the wing section and to correlate these in the temporal, spectral and spatial domains with full-field acoustic/flow dynamics. This opens the possibility for enhanced vibroacoustic measurement campaigns where causality between the surface velocity modes and the radiated acoustic fields can be determined with clarity.

Acknowledgments

The authors acknowledge partial support of the studies outlined in this paper by NASA Langley Research Center through contracts No. NNX15CL70P and No. NNX14CL73P.

References

[1] Burroughs, C., Carroll, G. P., Cuschiera, J. M., "Evaluation of Structure-borne Noise Prediction Techniques", *Noise-Con 94*, Ft. Lauderdale, FL, 1994, pp. 541-544.

[2] Langley, R. S., and Fahy, F. J., "High-Frequency Structural Vibration", *Advanced Applications in Acoustics, Noise, and Vibration*, Spon Press, 2004, pp. 490-529.

[3] Cabell, R., Klos, J., Buehrle, R., Schiller, N., "Vibroacoustic Response Data of Stiffened Panels and Cylinders", *Noise-Con 2008*, Dearborn, MI, 2008.

[4] Chelliah, K., Raman, G., Muehleisen, R.T., "An experimental comparison of various methods of nearfield acoustic holography", *Journal of Sound and Vibration*, Vol. 403, 2017, pp. 21-37.

[5] Mukwevho, T., Jordaan, J., Noel, G., "Advanced Beamforming Techniques for Acoustic Source Localization", *IEEE AFRICON*, 2009, pp. 1-6.

[6] Benerjee, S., Dwivedi, V.V. "Comparative analysis of adaptive beam forming techniques", *Progress in Intelligent Computing Techniques: Theory, Practice, and Applications*, Springer, 2017, pp. 357-364.

[7] Merino-Martinez, R., Sijtsma, P., et al., "A Review of Acoustic Imaging Methods Using Phased Microphone Arrays", *CEAS Aeronautical Journal*, Vol. 10, 2019, pp. 197-230.

[8] Kilpatrick, J., Apostol, A., Markov, V., "Method and System for Conformal Imaging Vibrometry", U.S. Patent No. 9,274,135 B2, March 1, 2016.

[9] Kilpatrick, J., Apostol, A., Markov, V., "Design and applications of a high-speed Doppler imaging vibrometer", *Proc. SPIE* Vol. 7791, 2010, pp.77910B.

[10] Abado Sh., Gordeyev, S., Jumper E. J. "Two-dimensional high-bandwidth Shack-Hartmann wavefront sensor: design guidelines and evaluation testing", *Optical Engineering*, Vol. 49, 2010, pp. 064403-1 - 064403-9

[11] Radosevich, C. J., Wilcox C. C. Wilcox, Dayton, D.C. et al., "Dual wavefront sensing design for supersonic wind tunnel experiments", *Proc. SPIE* 10772, (2018) pp.1077209-1 - 1077209-9;